

Ellagic acid: A potent glyoxalase-I inhibitor with a unique scaffold

NIZAR A. AL-SHAR¹*,
QOSAY A. AL-BALAS¹
MOHAMMAD A. HASSAN¹
TAMAM M. EL-ELIMAT¹
GHAZI A. ALJABAL¹
AMMAR M. ALMAAYTAH²

¹ Department of Medicinal Chemistry
and Pharmacognosy, Faculty of
Pharmacy, Jordan University of Science
and Technology, P.O. Box 3030
Irbid 22110, Jordan

² Department of Pharmaceutical
Technology, Faculty of Pharmacy, Jordan
University of Science and Technology
P.O. Box 3030, Irbid 22110, Jordan

Accepted March 21, 2020
Published online April 15, 2020

The glyoxalase system, particularly glyoxalase-I (GLO-I), has been approved as a potential target for cancer treatment. In this study, a set of structurally diverse polyphenolic natural compounds were investigated as potential GLO-I inhibitors. Ellagic acid was found, computationally and experimentally, to be the most potent GLO-I inhibitor among the tested compounds which showed an IC_{50} of 0.71 $\mu\text{mol L}^{-1}$. Its binding to the GLO-I active site seemed to be mainly driven by ionic interaction *via* its ionized hydroxyl groups with the central Zn ion and Lys156, along with other numerous hydrogen bonding and hydrophobic interactions. Due to its unique and rigid skeleton, it can be utilized to search for other novel and potent GLO-I inhibitors *via* computational approaches such as pharmacophore modeling and similarity search methods. Moreover, an inspection of the docked poses of the tested compounds showed that chlorogenic acid and dihydrocaffeic acid could be considered as lead compounds worthy of further optimization.

Keywords: ellagic acid, glyoxalase-I, zinc-binding, anticancer, molecular docking, MM-GBMV

The glyoxalase system is a ubiquitous detoxifying pathway in which reactive metabolic aldehydes are detoxified. It consists of two consecutive thiol-dependent zinc coordinating metalloenzymes, namely, glyoxalase I (GLO-I) and glyoxalase II (GLO-II) (1). The detoxification is accomplished by converting the toxic glycolysis by-product methylglyoxal to S-D-lactoyl-glutathione (SLG). The process proceeds by GLO-I catalyzed isomerization of thiohemiacetal, which is formed spontaneously from methylglyoxal and GSH, into S-D-lactoyl-glutathione. Then, GLO-II catalyzes the hydrolysis of SLG releasing the non-toxic D-lactic acid and regenerating GSH cofactor (1, 2). Since the accumulation of methylglyoxal and similar oxoaldehydes is deleterious to cell viability, targeting the glyoxalase system with potent inhibitors presents a potential goal especially for the treatment of oncotic disorders where the cellular production of these toxic metabolites is abnormally high (3–7).

* Correspondence; e-mail: nashari@just.edu.jo

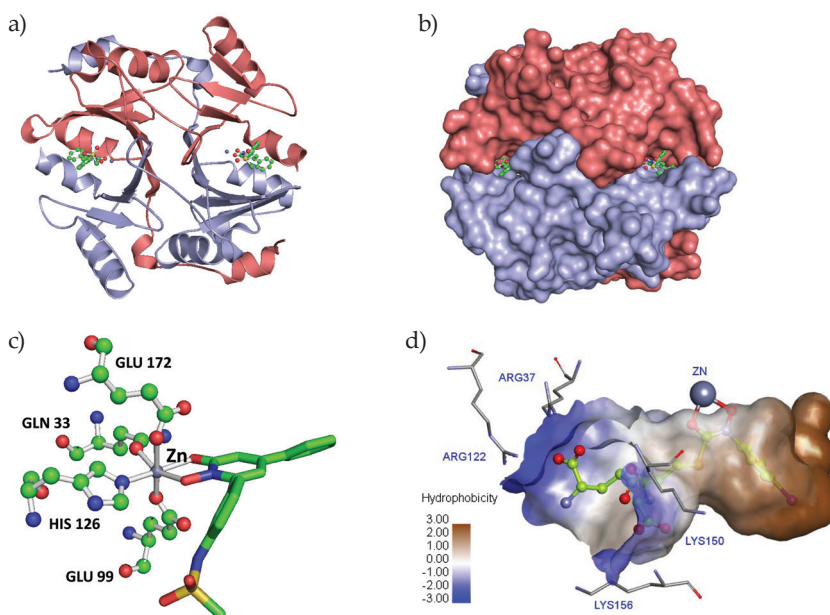


Fig. 1. a) The human GLO-I crystal structure (PDB code 3W0T). The protein is shown in cartoon representation where chain A and chain B are colored in deep salmon and light blue, resp. The HPU is shown in balls and sticks, and Zn²⁺ ions as purple spheres; b) Surface depiction of the GLO-I enzyme showing the location of the binding site at the dimer interface; c) A close-up view of the active site showing the coordination geometry of the Zn²⁺ ion and the amino acid residues (ball and stick) and HPU (sticks) involved in this coordination; d) Surface depiction of the GLO-I active site (PDB code 1QIN) illustrating the three major binding regions. The hydrophobic pocket is colored brown, the zinc atom is shown as a purple sphere, and the positively charged mouth is colored blue with relevant amino acid residues are shown as sticks. The co-crystallized ligand that coordinates the Zn atom is in balls and sticks with green carbon atoms.

Structurally, the GLO-I enzyme is a homodimeric mononuclear zinc-coordinating metalloenzyme with each monomer comprising 183 residues, and the active site is located at the interface of the two chains. The central zinc ion within the active site coordinates 4 amino acid residues from both chains (8) (Fig. 1a,b). When co-crystallized with HPU (*N*-hydroxypyridone derivative, PDB entry code 3W0T), two additional dative bonds between the zinc ion and the ligand align the geometry of coordination with a perfect octahedral (Fig. 1c). Moreover, the active site of the GLO-I enzyme can be divided into a deep hydrophobic region, a central zinc atom, and a positively charged mouth (Fig. 1d).

Our research group has been targeting the GLO-I enzyme for almost a decade where a large number of diverse compounds have been designed, synthesized and screened (6, 9–15). In this study, we build on our previous work of searching for potent GLO-I inhibitors of which natural flavonoids had demonstrated superior affinity to the GLO-I active site, thus serving as a potent inhibitor for the bioconversion of methylglyoxal and as potential anticancer agents (9, 11, 12). Previously, we investigated the structure-activity relationship of flavonoids as potential GLO-I inhibitors and found that the multiple electro-

negative polar oxygen centers are expected to coordinate well with the positively charged zinc ion. In addition, their nearly rigid skeleton and their geometry that fit the enzyme hydrophobic pocket had explained their tight binding to the GLO-I active site (11). The accumulated evidence of the inhibitory potential of polyphenolic natural compounds, such as flavonoids, against the GLO-I enzyme, has encouraged us to proceed further in this direction. Therefore, a set of structurally diverse polyphenolic natural compounds that have never been tested against GLO-I enzyme were selected to further validate and investigate, computationally and experimentally, the impact of ionizability and structural rigidity of polyphenolic compounds on their GLO-I inhibitory potential. Moreover, we aimed to search for new scaffolds of natural compounds that can be of therapeutic potential as potent GLO-I inhibitors.

EXPERIMENTAL

Materials and software

Seven of the selected compounds were purchased from Combi-Blocks, Inc. (USA), Sigma-Aldrich (USA), Acros Organics (Belgium), Santa Cruz Biotechnology, Inc. (USA), and Toronto Research Chemicals Inc. (Canada). Isosilybin A, silychristin, and isosilychristin were a kind gift from Dr. Nicholas H. Oberlies, the University of North Carolina at Greensboro (USA).

In vitro assay of the selected compounds was performed against the human recombinant GLO-I (rhGLO-I), *E. coli*-derived Ala2-Met184, with an *N*-terminal Met and 6-His tag (R&D Systems® Corporation, USA) using a double-beam UV-Vis spectrophotometer (Biotech Engineering Management Co. Ltd. Cyprus).

Preparation of the GLO-I crystal structure was performed using Discovery Studio (DS) 2017 (Dassault Systèmes BIOVIA, Discovery Studio Modeling Environment, Release 2017, Dassault Systèmes, 2016, USA). Solvation of the GLO-I enzyme was performed using the Solvate protocol within DS. Minimization of the solvated GLO-I model was performed using the smart minimizer algorithm within the Minimization protocol that uses the CHARMM force field (16) implemented in DS MD protocols. QM-based atomic charge calculations were performed using the Calculate Energy (DFT) protocol within DS. Molecular docking was performed using CDOCKER docking protocols within DS. MM-GBMV binding energy calculations were performed using calculate binding energy protocol in DS (17). Presentation quality images were generated using PyMOL (The PyMOL Molecular Graphics System, Version 0.99 Schrödinger, LLC) and DS. GraphPad Prism (GraphPad Software: La Jolla (CA), USA) was used for calculation of the % of enzyme inhibition and IC_{50} values.

Ligands preparation

Using ChemDraw, studied compounds were drawn and geometrically optimized. Using the DS standard Prepare Ligands protocol, pH based ionization was performed within a pH range of 7.0–7.6, and more importantly, different chemical tautomers were generated. In this study, multiple tautomeric configurations were used in order to account for receptor-induced tautomerization. For ellagic acid and myricetin, manual ionization was performed to match the ionization states reported in the literature.

Preparation of the GLO-I enzyme

DS was used to prepare the crystal structure of the enzyme which was obtained from the Protein Data Bank (PDB). The PDB holds six records of GLO-I crystal structures with accession codes 3VW9, 3W0T, 3W0U, 1QIN, 1QIP, and 1FRO. The 3W0T crystal, which has the highest resolution (1.35 Å), was selected which corresponds to two units of GLO-I complexed with *N*-hydroxypyridone derivative inhibitor (HPU). The Protein Report tool within DS was used to check the quality of the crystal structure for missing loops, incomplete residues and alternate conformations. Then, one of the dimer units was deleted and the structure was cleaned using the Prepare Protein protocol within DS to correct connectivity and bond order, standardize atom names, protonate protein at pH of 7.4, and keep one set of coordinates for residues with alternate conformation. There were seven amino acid residues with alternate conformation that are distant from the active site and have subtle conformational differences. Later, all ligands were deleted in order to solvate and minimize the apo-enzyme. The co-crystallized waters were not deleted in order not to create holes within the protein that will not be filled upon solvation. Finally, the structure was typed using the Simulation Tools by applying the CHARMM force field and it was ready for further modeling steps.

Solvation and minimization of the GLO-I enzyme

The prepared enzyme was explicitly solvated using a pre-equilibrated truncated octahedral cell of TIP3 water (18) with a 7.0 Å minimum distance from the cell boundary. Then, it was neutralized by adding NaCl counterions at 0.145 mol L⁻¹ ionic strength. Finally, the solvated system was minimized using the smart minimizer algorithm within the Minimization protocol. The smart minimizer performs 1000 steps of Steepest Descent, followed by Conjugate Gradient minimization (19), and herein, 5000 steps of conjugate gradient minimization were used with a root mean square (RMS) gradient of 0.1 kcal mol⁻¹ Å⁻¹. The minimization step was subdivided into three stages in order to relax the system and remove all potential clashes between the protein and the solvent without creating distortions in the overall protein structure. In the first minimization stage, all heavy atoms were constrained, then only backbone atoms were constrained, and in the third stage all constraints were removed to allow free motion of the entire system.

Molecular docking and calculation of binding energies

The CDocker Docking protocol (20) was employed to dock the selected compounds into the active site of the GLO-I enzyme using default parameters with a final full potential minimization step. Finally, the binding free energies of all docked poses were calculated using the Calculate Binding Energy protocol, where implicit solvation using the Generalized Born with Molecular Volume (MM-GBMV) model was applied (17).

In vitro enzyme assay

Human recombinant GLO-I (rhGLO-I) was used in the *in vitro* assay to measure the biological activity of selected compounds against GLO-I enzyme as previously detailed (9–11). Briefly, the enzyme was reconstituted in our lab and aliquots were stored at -70 °C.

Tested compounds were dissolved in DMSO, the final concentration of DMSO in the assay mixture was 0.5 %. A sodium phosphate assay buffer was used with a pH of 7.0–7.2. The substrate mixture was prepared by mixing the methylglyoxal solution with assay buffer. Finally, the tested compounds were mixed with the assay buffer, GLO-I enzyme, and substrate solution mixture in a cuvette making a final compound concentration of 50 $\mu\text{mol L}^{-1}$, then screened at $\lambda_{\text{max}} = 240 \text{ nm}$ for 200 s at 37 °C. Each concentration was measured in triplicate. The IC_{50} values of the active compounds were calculated.

RESULTS AND DISCUSSION

Compounds selection

The aim of this study was to search for new scaffolds that can be utilized in designing more potent and selective GLO-I inhibitors and to further investigate the impact of ionizability and structural rigidity of polyphenolic compounds on their GLO-I inhibitory potential. Therefore, a set of structurally diverse polyphenolic natural compounds were selected for *in silico* evaluation. The set included three flavonolignans: isosylibin A, silychristin and isosilychristin; (–)-epicatechin (a flavonoid); and maesopsin (a flavonoid with a benzofuranone scaffold). These compounds are lacking the C2-C3 olefinic bond in their flavonoid skeleton that was deemed critical for the activity (11). The compounds were selected to further test the validity of our previous SAR conclusions. Additionally, cardamomin, a chalcone, and dihydrocaffeic and chlorogenic acids that are hydroxycinnamic acid derivatives were also included. All of the three compounds are lacking the 3-ring system of flavonoids, yet, they are poly-hydroxylated phenols with a carboxylate moiety (not cardamomin) that is known to be a good zinc binder. Moreover, they have some structural resemblance to *trans*-stilbenes of which piceatannol has been proved to have good GLO-I inhibitory activity (21). The last compound selected was ellagic acid, a symmetrical dimeric derivative of gallic acid, which is a polyphenol with a unique rigid and planar structural scaffold.

Ligands preparation

The ionization state of a ligand affects its binding interactions with the GLO-I enzyme. Since most of the selected compounds are polyphenols that have different ionization states at different pHs it is important to verify the output of ligand preparation step. Therefore, the prepared ligands were inspected in order to check how the Prepare Ligands protocol performed the ionization step in the specified pH range.

In the pH range of 7.0–7.6 the Prepare Ligand protocol generated two ionization states of ellagic acid, unionized, and ionized with a net charge of –1, based on the hydroxyl group ionization on equivalent C2 and C7 carbon atoms. For myricetin, the Prepare Ligand protocol generated only one ionization state with a net charge of –2 (Fig. 2). However, the pK_a values of ellagic acid are reported to be ($pK_{a1} = 5.42 \pm 0.01$ and $pK_{a2} = 6.76 \pm 0.02$) in aqueous media (22, 23), which are lower than that of myricetin (6.63 ± 0.09) (24). Moreover, Simic *et al.* (22) have reported that in the pH range of 4.8–7.6, all three ellagic acid forms exist (unionized, monoanion and dianion), while at pH higher than 7.6 the dianion predominates (22). Nonetheless, there are some controversies about the first deprotonable OH group (the most acidic) in ellagic acid: whether they are the (C3-OH, C8-OH) or the (C2-

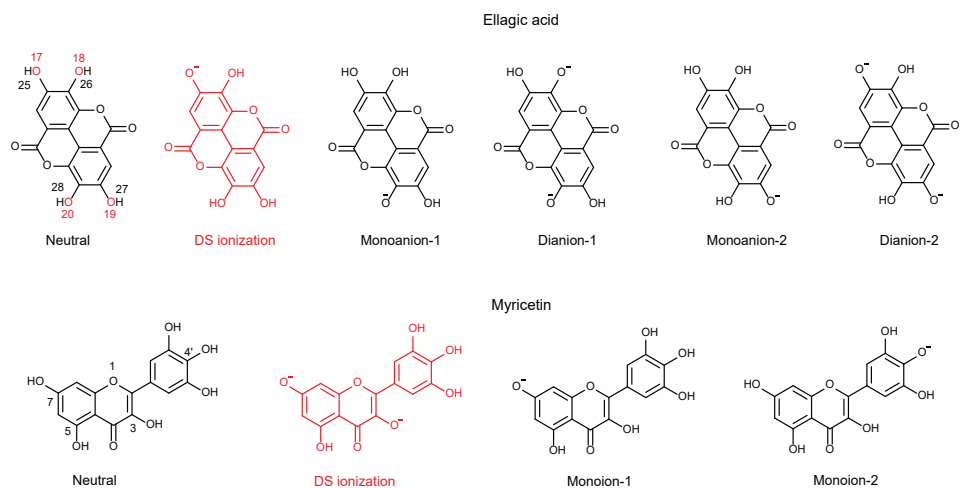


Fig. 2. The different ionization states of ellagic acid and myricetin as reported in the literature (22–24) (colored black) compared to those obtained from the Prepare Ligand protocol in DS (colored red).

OH, C7-OH) (23, 25, 26). Further, it has been predicted that the physiological net charges of ellagic acid and myricetin are -2 and -1 , resp. (as per DrugBank, <https://www.drugbank.ca>), which agrees with the reported pK_a values of the two compounds and the ionization forms of ellagic acid at different pHs. Moreover, it has been reported that for flavones such as myricetin the most acidic site is the 4'-hydroxyl group (27), however, in other reports the 7-hydroxyl group was considered the most favored deprotonation site (28).

Therefore, in order to enhance the accuracy of the docking results, all possible physiological ionization states of the two compounds were manually prepared based on data reported in the literature (22–24, 27–29) (Fig. 2). Moreover, quantum mechanics (QM) calculations were performed for ellagic acid and myricetin to confirm the most likely ionization form for each compound (Table I). Then, different tautomers of the two edited compounds were generated using Prepare Ligands protocol and were then docked into the GLO-I active site along with other prepared compounds in the selected set.

Table I. QM-based partial charges of the most ionizable hydrogens in ellagic acid and myricetin

Compound	Atom name and ID ^a	Partial charges (DMol ³)	
		Mulliken method	Hirshfeld method
Ellagic acid	H26 and H28	+ 0.333	+ 0.181
	H25 and H27	+ 0.328	+ 0.205
Myricetin	H of the C7-OH	+ 0.362	+ 0.210
	H of the C4'-OH	+ 0.357	+ 0.200

QM – quantum mechanics

^a For atom numbering refer to Fig. 2.

QM calculations were performed using the Calculate Energy (DFT) protocol within DS which performs density functional QM calculation using DMol³ (29). Default parameters were used except for the function for which the hybrid B3LYP functional was used, the quality of calculations was set to fine and using water as the solvent. The atomic charges were calculated using the Mulliken (25) and the Hirshfeld methods (26). QM results were similar to those reported in the literature where the most ionizable hydroxyl group in ellagic acid was variable depending on the QM method, yet, the values of the partial charges were quite close. For myricetin, the C7-OH seems to be the most ionizable group with little difference from the C4'-OH.

Preparation of the GLO-I model

The initial coordinates of GLO-I were obtained from X-ray crystallography, which usually suffers artifacts such as crystal packing. Therefore, in order to generate a relaxed and more realistic protein conformation, the prepared apo-enzyme was solvated and minimized. The prepared apo-GLO-I model was explicitly solvated with a TIP3P water truncated octahedral solvation cell in order to better mimic the experimental conditions. Then, the minimization of the solvated system relieved crystal strain and drove the system into a local minimum. Examination of the six solvated crystal complexes of GLO-I enzyme available in the PDB showed no direct involvement of structural water in ligand binding, hence, all water molecules and counterions, NaCl, were deleted from the minimized solvated system and the protein was ready to be used in subsequent molecular docking.

Molecular docking and calculation of binding energies

Molecular docking is a valuable and frequently used method in structure-based drug design (SBDD). This is due to its ability to predict the binding configuration of a docked ligand and to estimate its binding affinity within the virtual complex (30). Among the limitations of current scoring functions that affect binding affinity prediction is the limited treatment of the solvation effect (31). One of the ways to alleviate this problem and improve the accuracy of binding affinity prediction is to apply physics-based scoring, *e.g.*, MM-PB/SA, MM-GB/SA, and MM-GBMV (MM stands for molecular mechanics, PB and GB for Poisson-Boltzmann and Generalized Born, resp., SA for solvent-accessible surface area, and MV for molecular volume) (32).

CDOCKER, which is a grid-based molecular docking algorithm that utilizes the CHARMM force field (17, 20), was used in this study to dock the selected compounds into the active site of the GLO-I enzyme. However, it is customary to validate the docking method (the perception of the active site by the docking algorithm, and whether the active site is well defined or not) before taking it forward (docking the set of selected compounds) (33). This was achieved by redocking the co-crystallized ligand into the defined binding site and comparing the resultant poses with the co-crystallized ligand conformation, hence, testing the accuracy of the docking algorithm in recapitulating the co-crystallized ligand pose. The docking results were in excellent agreement with the co-crystallized HPU pose with a root mean square deviation (RMSD) of 0.896 Å. Afterward, the set of selected compounds were docked into the active site of the GLO-I enzyme using CDOCKER algorithm with a final refinement step using grid-based simulated annealing and a full-force field minimization (Table II). The docked poses of the studied compounds were

ranked based on their –CDOCKER energy, which corresponds to ligand-receptor interaction energy plus ligand strain, where higher values correspond to better binding affinity. The (–)CDOCKER energy scores were ranging from 14.65 kcal mol⁻¹ for isosilychristin to 55.39 kcal mol⁻¹ for myricetin.

The CDOCKER scoring function is a force field-based function (*i.e.*, electrostatic and van der Waal interaction energies are summed up to total interaction energy based on which a ligand is scored and ranked) and is reported to have a docking success rate of 74 % (20), yet, it does not account for solvation/desolvation energy, entropy, or ΔG of binding. Therefore, a more rigorous method for estimating the binding energy of docked poses was used. Here, we implemented the MM-GBMV implicit solvent model, embedded within the calculate binding energy protocol in DS, to account for solvation/desolvation energy which improves the accuracy of ligand-protein binding affinity prediction (17, 32) (Table II). Prior to running the MM-GBMV protocol all docked poses were *in situ* minimized using the *In Situ* Ligand Minimization protocol in DS using default parameters except for the number of smart minimizer steps which was set to 5000. The binding free energy for a protein-ligand complex can be calculated from the free energies of the complex, the protein, and the ligand according to the following equation.

$$Energy_{Binding} = Energy_{Complex} - Energy_{Ligand} - Energy_{Protein}$$

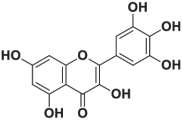
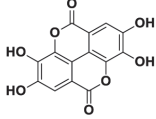
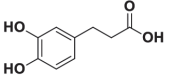
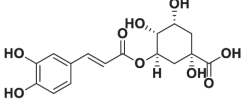
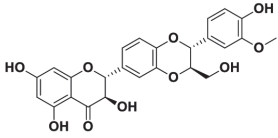
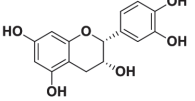
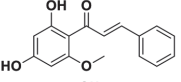
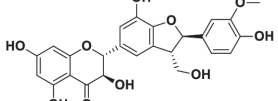
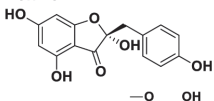
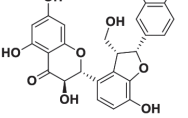
Interestingly, the MM-GBMV calculations showed that ellagic acid had the highest binding energy score with 84.01 kcal mol⁻¹, which is higher than that of myricetin, the positive control used in this study. The (–)binding free energies of the selected compounds were ranging from 4.30 kcal mol⁻¹ for maesopsin to 84.01 kcal mol⁻¹ for ellagic acid. The (–)CDOCKER scores and binding energy values of the compounds (–)-epicatechin, cardamomin, silychristin, maesopsin, and isosilychristin (compounds 6–10) were ranging from 14.65 to 29.81 kcal mol⁻¹ and 7.32 to 24.41 kcal mol⁻¹, resp., suggesting these compounds to be inactive or weakly active. Nonetheless, compounds 6–10, which are expected to be inactive or weakly active, were biologically tested in order to assess the validity and accuracy of the applied *in silico* approach, when comparing predictions with experimental results. They were also needed to support previously drawn structure-activity relationship (SAR) of flavonoids as GLO-I inhibitors.

In vitro enzyme assay

The biological activities of the selected compounds against the GLO-I enzyme were evaluated using an *in vitro* enzyme assay. The selected compounds were initially screened at 50 $\mu\text{mol L}^{-1}$ concentration and their percent of GLO-I inhibition was measured relative to myricetin (the positive control) (Table II).

The initial screening of the tested compounds showed that ellagic acid has the most potent inhibitory activity with GLO-I inhibition of 97.5 %, in perfect agreement with the MM-GBMV results, followed by chlorogenic acid and (–)-epicatechin that showed activities around one-half that of ellagic acid (52.3 and 45.5 %, resp.). This result demonstrates that the hydroxylation pattern and structural rigidity of ellagic acid could be a key factor for its pronounced activity against the GLO-I enzyme. Furthermore, the experimental results agree with the *in silico* ones regarding compounds' expected activities; more details will be presented in the correlation section.

Table II. Chemical structures of the studied compounds along with their CDOCKER energy scores, (–) binding energy score and GLO-I inhibition (%)^{b,c}

No.	Chemical structure	Name	(–)CDE ^a	(–)BE	GLO-I inhibition (%) ^{b,c}
1		Myricetin	55.39	69.95	91.3 ± 2.9
2		Ellagic acid	48.03	84.01	97.5 ± 1.6
3		Dihydrocaffeic acid	43.24	31.99	17.4 ± 3.3
4		Chlorogenic acid	37.78	16.45	52.3 ± 7.3
5		Isosilybin A	29.94	31.33	28.4 ± 11.9
6		(–)-Epicatechin	29.81	7.32	45.5 ± 4.8 ₅
7		Cardamonin	26.77	24.41	32.5 ± 3.9
8		Silychristin	24.81	21.02	6.7 ± 5.8
9		Maesopsin	16.68	4.30	0.0 ₄ ± 0.0 ₃
10		Isosilychristin	14.65	22.41	6.4 ± 11.0

(–)BE – the negative value of the binding free energy calculated using the MM-GBMV model, (–)CDE – the negative value of CDOCKER energy

^a Tested compound are sorted in a decreasing order of their (–)CDOCKER energy scores.

^b Concentration: 50 μmol L⁻¹.

^c The data represents the mean ± SD of three independent experiments.

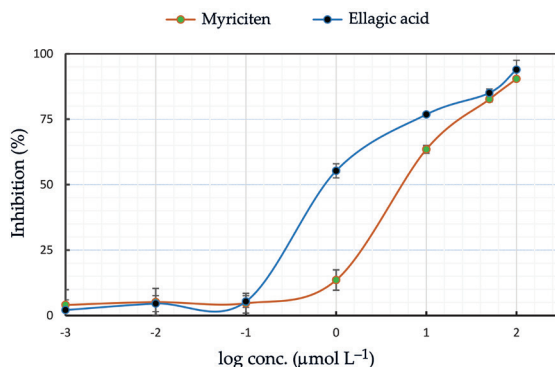


Fig. 3. Dose-response curves and IC_{50} values of human GLO-I inhibition for ellagic acid compared to myricetin (the positive control). The shown results correspond to the mean \pm SD of three independent experiments.

Following the determination of the percent of GLO-I inhibition by the tested compounds, the dose-dependency of GLO-I inhibition by ellagic acid (**2**) was measured in order to determine its IC_{50} value (Fig. 3). The IC_{50} of ellagic acid was found to be $0.71 \mu\text{mol L}^{-1}$, about eightfold lower than that of myricetin (**1**) with IC_{50} of $5.44 \mu\text{mol L}^{-1}$. The percent of GLO-I inhibition by other compounds was ranging from 0.04 to $52.33 \mu\text{mol L}^{-1}$. Therefore, they were considered weakly active or inactive and the determination of their IC_{50} values was not pursued.

Correlation between the *in silico* and experimental results

The correlation between the *in silico* and experimental results was calculated using the Pearson correlation coefficient (34). The correlation coefficient (R) between the (-)CDOCKER energy scores using the solvated minimized enzyme and the % of GLO-I inhibition values for the tested compounds was found to be 0.84. This high value of R indicates a strong positive correlation, which means that high (-)CDOCKER scores, corresponding to high binding affinity, are paired with high % of GLO-I inhibition. Similarly, the correlation between the (-)binding free energy scores and the % of GLO-I inhibition values was 0.81, meaning that high binding energy values (stable complex) are paired with high % of GLO-I inhibition. Note that the CDOCKER and the Binding energy scores are reported as negative values (Table II), therefore a higher positive value indicates a more favorable binding.

Analysis of the docked poses of tested compounds

Compounds **5–10** were expected, based on the *in silico* results, and on our previously proposed SAR of flavonoids as GLO-I enzyme inhibitors (not **7**, being lacking the C2-C3 olefinic bond and/or the C4-keto functionalities) to be inactive or weakly active. The *in silico* results were in excellent agreement with the *in vitro* ones for these compounds and supported our previous SAR conclusions. For example (-)-epicatechin is structurally similar to quercetin, an excellent GLO-I inhibitor, however, the lack of the C2-C3 olefinic bond and the C4-keto functionalities has hampered its activity.

moiety is establishing strong interactions with His126 and Arg37 that were absent in the parent chlorogenic acid making it a plausible analog (Fig. 4b).

Dihydrocaffeic acid (3), on the other hand, can be considered as an efficient fragment. It is the smallest compound in the tested set, and yet, forms interesting interactions with zinc ion and the hydrophobic pocket. Structural optimization *via* evolution to a larger structure, for example, that can reach and interact with Arg37, besides the interactions it forms with the zinc ion and the hydrophobic pocket, could lead to a more potent derivative (Fig. 4a).

The binding interactions of ellagic acid with GLO-I active site

Interestingly, the *in silico* results had shown that ellagic acid (2) is the most active compound among the selected series which was approved by the *in vitro* biological assay. The excellent activity of ellagic acid, its novel scaffold and the numerous studies that highlighted its biological functions and benefits to human health (35, 36), necessitate further exploration of the binding mode of this promising compound within the GLO-I active site that could aid the design of more potent GLO-I inhibitors.

As stated previously, in order to investigate the effect of different ionization states and tautomeric forms of ellagic acid on its GLO-I binding affinity different tautomers with all possible physiological ionization states were prepared and docked into the GLO-I active site. All of the 10 top-ranked poses of ellagic acid based on (-)CDOCKER energy scores correspond to the ionized form of the compound, of which seven poses correspond to the

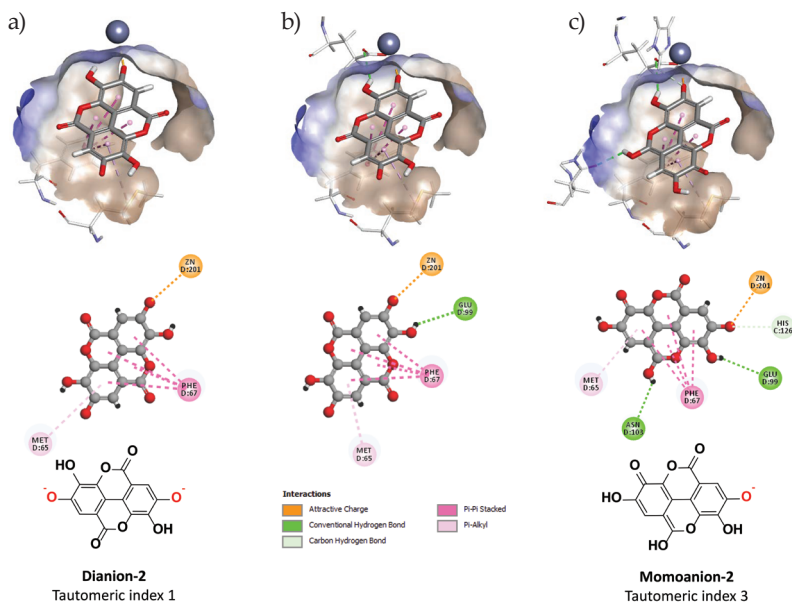


Fig. 5. The three top-ranked docked poses of ellagic acid based on -CDOCKER energy scores. a) Top-ranked pose (dianion-2); b) 2nd top-ranked pose (dianion-2); c) 3rd top-ranked pose (monoanion-2). Depictions of panels are as in Fig. 4.

the enzyme equally well. This agrees with the findings of Simic *et al.* (22) who reported that in the pH range of 4.8–7.6 all three ellagic acid ionization forms exist.

However, the dianion-2 was the predominant ionization form of ellagic acid and is the one that showed the highest (–)CDOCKER and (–)binding energy scores to which the pronounced activity of the compound is likely to be attributed. Collectively, the pronounced activity and potency of ellagic acid are attributed to its numerous interactions formed with the GLO-I enzyme besides its shape and geometry which ultimately result in a complete blockade of the active site.

CONCLUSIONS

The aim of this study was to search for a potent GLO-I inhibitor. The present computational work revealed that ellagic acid could lead to an energetically stable complex and thus favorable binding with GLO-I enzyme which was supported and confirmed by the *in vitro* enzyme assay that showed an IC_{50} value of ellagic acid of $0.71 \mu\text{mol L}^{-1}$. Binding of ellagic acid to the GLO-I active site seems to be mainly driven by attractive interaction between its dianion form and the Zn ion and Lys156 along with numerous hydrogen bonding and hydrophobic interactions. Based on the current evidence, ellagic acid can be utilized, due to its unique and rigid scaffold, to search for other novel and potent GLO-I inhibitors *via* computational approaches such as pharmacophore modeling and similarity search methods. Besides, chlorogenic acid and dihydrocaffeic acid can be considered as lead compounds that are worthy of optimization towards designing more potent GLO-I inhibitors. Moreover, it is important to check the accuracy of used algorithms in preparing ligands (ionization in our case) before proceeding further in modeling steps, since inaccurate preparation could result in misleading results. Finally, given the excellent activity of ellagic acid and its cost-effectiveness relative to myricetin it could be used as a positive control in GLO-I enzyme inhibition assays instead of myricetin.

Acknowledgment. – The authors wish to thank the Deanship of Scientific Research at Jordan University of Science and Technology for financial support.

Abbreviations, acronyms, symbols. – BE – the negative value of the binding free energy, (–)CDE – the negative value of CDOCKER energy, DFT – density functional theory, DS – discovery studio, GBMV – generalized Born with molecular volume, GBSA – generalized Born with solvent-accessible surface area, GLO – glyoxalase, GSH – glutathione, MM – molecular mechanics, PBSA – Poisson Boltzmann with non-polar Surface Area, PDB – protein data bank, QM – quantum mechanics, RMSD – root mean square deviation, SBDD – structure-based drug design, SLG – S-D-lactoyl-glutathione.

REFERENCES

1. P. J. Thornalley, The glyoxalase system: new developments towards functional characterization of a metabolic pathway fundamental to biological life, *Biochem. J.* 269 (1990) 1–11.
2. M. Sousa Silva, R. A. Gomes, A. E. N. Ferreira, A. P. Freire and C. Cordeiro, The glyoxalase pathway: the first hundred years... and beyond, *Biochem. J.* 453 (2013) 1–15; <https://doi.org/10.1042/bj20121743>
3. A. Rulli, L. Carli, R. Romani, T. Baroni, E. Giovannini, G. Rosi and V. Talesa, Expression of glyoxalase I and II in normal and breast cancer tissues, *Breast Cancer Res. Treat.* 66 (2001) 67–72; <https://doi.org/10.1023/a:1010632919129>
4. E. Mearini, R. Romani, L. Mearini, C. Antognelli, A. Zucchi, T. Baroni, M. Porena and V. N. Talesa, Differing expression of enzymes of the glyoxalase system in superficial and invasive bladder carcinomas, *Eur. J. Cancer* 38 (2002) 1946–1950; [https://doi.org/10.1016/S0959-8049\(02\)00236-8](https://doi.org/10.1016/S0959-8049(02)00236-8)

5. P. J. Thornalley, The glyoxalase system in health and disease, *Mol. Aspects Med.* **14** (1993) 287–371; [https://doi.org/10.1016/0098-2997\(93\)90002-U](https://doi.org/10.1016/0098-2997(93)90002-U)
6. Q. Al-Balas, M. Hassan, B. Al-Oudat, H. Alzoubi, N. Mhaidat and A. Almaaytah, Generation of the first structure-based pharmacophore model containing a selective “zinc binding group” feature to identify potential glyoxalase-I inhibitors, *Molecules* **17** (2012) 13740–13758; <https://doi.org/10.3390/molecules171213740>
7. A. N. Al-Shar'i, M. Hassan, Q. Al-Balas and A. Almaaytah, Identification of possible glyoxalase II inhibitors as anticancer agents by a customized 3D structure-based pharmacophore model, *Jordan J. Pharm. Sci.* **8** (2015) 83–103.
8. A. D. Cameron, B. Olin, M. Ridderström, B. Mannervik and T. A. Jones, Crystal structure of human glyoxalase I - evidence for gene duplication and 3D domain swapping, *EMBO J.* **16** (1997) 3386–3395; <https://doi.org/10.1093/emboj/16.12.3386>
9. Q. A. Al-Balas, M. A. Hassan, N. A. Al-Shar'i, N. M. Mhaidat, A. M. Almaaytah, F. M. Al-Mahasneh, and I. H. Isawi, Novel glyoxalase-I inhibitors possessing a “zinc-binding feature” as potential anti-cancer agents, *Drug Des. Dev. Ther.* **10** (2016) 2623–2629; <https://doi.org/10.2147/DDDT.S110997>
10. Q. A. Al-Balas, A. M. Hassan, G. A. Al Jabal, N. A. Al-Shar'i, A. M. Almaaytah and T. El-Elimat, Novel thiazole carboxylic acid derivatives possessing a “zinc binding feature” as potential human glyoxalase-I inhibitors, *Lett. Drug Des. Discov.* **14** (2017) 1324–1334; <https://doi.org/10.2174/1570180814666170306120954>
11. Q. A. Al-Balas, M. A. Hassan, N. A. Al-Shar'i, T. El-Elimat and A. M. Almaaytah, Computational and experimental exploration of the structure–activity relationships of flavonoids as potent glyoxalase-I inhibitors, *Drug Dev. Res.* **79** (2018) 58–69; <https://doi.org/10.1002/ddr.21421>
12. Q. Al-Balas, N. Al-Shar'i, K. Banisalman, M. Hassan, G. A. Jabal and A. Almaaytah, Design, synthesis and biological evaluation of potential novel zinc binders targeting human glyoxalase-I; A validated target for cancer treatment, *Jordan J. Pharm. Sci.* **11** (2018) 25–37.
13. Q. A. Al-Balas, M. A. Hassan, N. A. Al-Shar'i, G. A. Al Jabal and A. M. Almaaytah, Recent advances in glyoxalase-I inhibition, *Mini-Rev. Med. Chem.* **19** (2019) 281–291; <https://doi.org/10.2174/1389557518666181009141231>
14. N. A. Al-Shar'i, Q. A. Al-Balas, R. A. Al-Waqfi, M. A. Hassan, A. E. Alkhalifa and N. M. Ayoub, Discovery of a nanomolar inhibitor of the human glyoxalase-I enzyme using structure-based poly-pharmacophore modelling and molecular docking, *J. Comput. Aid. Mol. Des.* **33** (2019) 799–815; <https://doi.org/10.1007/s10822-019-00226-8>
15. N. A. Al-Shar'i, E. K. Al-Rousan, L. I. Fakhouri, Q. A. Al-Balas and M. A. Hassan, Discovery of a nanomolar glyoxalase-I inhibitor using integrated ligand-based pharmacophore modeling and molecular docking, *Med. Chem. Res.* **29** (2020) 356–376; <https://doi.org/10.1007/s00044-019-02486-3>
16. B. R. Brooks, C. L. Brooks, A. D. MacKerell, L. Nilsson, R. J. Petrella, B. Roux, Y. Won, G. Archontis, C. Bartels, S. Boresch, A. Caflisch, L. Caves, Q. Cui, A. R. Dinner, M. Feig, S. Fischer, J. Gao, M. Hodoscek, W. Im, K. Kuczera, T. Lazaridis, J. Ma, V. Ovchinnikov, E. Paci, R. W. Pastor, C. B. Post, J. Z. Pu, M. Schaefer, B. Tidor, R. M. Venable, H. L. Woodcock, X. Wu, W. Yang, D. M. York and M. Karplus, CHARMM: The biomolecular simulation program, *J. Comput. Chem.* **30** (2009) 1545–1614; <https://doi.org/10.1002/jcc.21287>
17. M. S. Lee, M. Feig, F. R. Salsbury and C. L. Brooks, New analytic approximation to the standard molecular volume definition and its application to generalized Born calculations, *J. Comput. Chem.* **24** (2003) 1348–1356; <https://doi.org/10.1002/jcc.10272>
18. P. Mark and L. Nilsson, Structure and dynamics of the TIP3P, SPC, and SPC/E water models at 298 K, *J. Phys. Chem. A* **105** (2001) 9954–9960; <https://doi.org/10.1021/jp003020w>
19. I. Štich, R. Car, M. Parrinell and S. Baroni, Conjugate gradient minimization of the energy functional: A new method for electronic structure calculation, *Phys. Rev. B* **39** (1989) 4997–5004; <https://doi.org/10.1103/PhysRevB.39.4997>
20. G. Wu, D. H. Robertson, C. L. Brooks and M. Vieth, Detailed analysis of grid-based molecular docking: A case study of CDOCKER—A CHARMM-based MD docking algorithm, *J. Comput. Chem.* **24** (2003) 1549–1562; <https://doi.org/10.1002/jcc.10306>

21. R. Takasawa, H. Akahane, H. Tanaka, N. Shimada, T. Yamamoto, H. Uchida-Maruki, M. Sai, A. Yoshimori and S.-i. Tanuma, Piceatannol, a natural trans-stilbene compound, inhibits human glyoxalase I, *Bioorg. Med. Chem. Lett.* **27** (2017) 1169–1174; <https://doi.org/10.1016/j.bmcl.2017.01.070>
22. A. Z. Simić, T. Ž. Verbić, M. N. Sentić, M. P. Vojić, I. O. Juranić and D. D. Manojlović, Study of ellagic acid electro-oxidation mechanism, *Monatsh. Chem. Chem. Mon.* **144** (2013) 121–128; <https://doi.org/10.1007/s00706-012-0856-8>
23. Z. Marković, D. Milenković, J. Đorović, J. M. Dimitrić Marković, B. Lučić and D. Amić, A DFT and PM6 study of free radical scavenging activity of ellagic acid, *Monatsh. Chem. Chem. Mon.* **144** (2013) 803–812; <https://doi.org/10.1007/s00706-013-0949-z>
24. Y. Yao, G. Lin, Y. Xie, P. Ma, G. Li, Q. Meng and T. Wu, Preformulation studies of myricetin: a natural antioxidant flavonoid, *Pharmazie* **69** (2014) 19–26.
25. R. S. Mulliken, Electronic population analysis on LCAO–MO molecular wave functions. I, *J. Chem. Phys.* **23** (1955) 1833–1840; <https://doi.org/10.1063/1.1740588>
26. F. L. Hirshfeld, Bonded-atom fragments for describing molecular charge densities, *Theor. Chim. Acta* **44** (1977) 129–138; <https://doi.org/10.1007/bf00549096>
27. H. F. P. Martins, J. P. Leal, M. T. Fernandez, V. H. C. Lopes and M. N. D. S. Cordeiro, Toward the prediction of the activity of antioxidants: experimental and theoretical study of the gas-phase acidities of flavonoids, *J. Am. Soc. Mass Spectrom.* **15** (2004) 848–861; <https://doi.org/10.1016/j.jasms.2004.02.007>
28. G. Günther, E. Berrios, N. Pizarro, K. Valdés, G. Montero, F. Arriagada and J. Morales, Flavonoids in microheterogeneous media, relationship between their relative location and their reactivity towards singlet oxygen, *PLoS ONE* **10** (2015) e0129749; <https://doi.org/10.1371/journal.pone.0129749>
29. B. Delley, An all-electron numerical method for solving the local density functional for polyatomic molecules, *J. Chem. Phys.* **92** (1990) 508–517; <https://doi.org/10.1063/1.458452>
30. T. Lengauer and M. Rarey, Computational methods for biomolecular docking, *Curr. Opin. Struct. Biol.* **6** (1996) 402–406; [https://doi.org/10.1016/S0959-440X\(96\)80061-3](https://doi.org/10.1016/S0959-440X(96)80061-3)
31. P. Ferrara, H. Gohlke, D. J. Price, G. Klebe and C. L. Brooks, Assessing Scoring functions for protein-ligand interactions, *J. Med. Chem.* **47** (2004) 3032–3047; <https://doi.org/10.1021/jm030489h>
32. S. Genheden and U. Ryde, The MM/PBSA and MM/GBSA methods to estimate ligand-binding affinities, *Expert Opin. Drug Discov.* **10** (2015) 449–461; <https://doi.org/10.1517/17460441.2015.1032936>
33. S. Matić, M. Jadrijević-Mladar Takač, M. Barbarić, B. Lučić, K. Gall Trošelj and V. Stepanić, The influence of in vivo metabolic modifications on ADMET properties of green tea catechins – In silico analysis, *J. Pharm. Sci.* **107** (2018) 2957–2964; <https://doi.org/10.1016/j.xphs.2018.07.026>
34. N. J. Cox, Speaking stata: Correlation with confidence, or Fisher's z revisited, *Stata J.* **8** (2008) 413–439; <https://ageconsearch.umn.edu/record/122603>
35. D. A. Vatter and K. Shetty, Biological functionality of ellagic acid: a review, *J. Food Biochem.* **29** (2005) 234–266; <https://doi.org/10.1111/j.1745-4514.2005.00031.x>
36. J. M. Landete, Ellagitannins, ellagic acid and their derived metabolites: A review about source, metabolism, functions and health, *Food Res. Int.* **44** (2011) 1150–1160; <https://doi.org/10.1016/j.foodres.2011.04.027>